DOI: 10.48011/asba.v2i1.1576

Modeling and identification of rotational joint driven by polymer fiber actuator

João R.C. de Araújo [*] Saulo O.D. Luiz [**]
Antonio M.N. Lima [***]

[*] *Graduate Program in Electrical Engineering - PPgEE/UFCG (e-mail: joao.araujo@ee.ufcg.edu.br)*
[**] *Electrical Engineering Department (DEE) Federal University of Campina Grande (UFCG) 58429-900, Campina Grande - PB Brazil, (e-mail: saulo@dee.ufcg.edu.br)*
[***] *Electrical Engineering Department (DEE) Federal University of Campina Grande (UFCG) 58429-900, Campina Grande - PB Brazil, (e-mail: amnlima@dee.ufcg.edu.br)*

Abstract: Coiled polymer actuators have the characteristic to generate power by contracting when heated under strain. This work presents a project of a rotational joint driven by such actuators. Furthermore, the thermomechanical model of the CPAs is identified by means of the least squares method. In addition, a model of the joint considering a viscous friction is suggested. Finally, the joint model is identified by means of a non linear optimization algorithm.

Keywords: Actuator, antagonistic, nylon, system identification.

1. INTRODUCTION

A phenomenon involving polymer fibers such as nylon and polyethylene was observed by Haines et al. (2014). These fibers perform a linear motion of contraction when, induced to helical form, are strained, and heated. It was observed they could contract up to 34% of their initial length and produce 5.3 kW of power per kilogram of fiber. In addition it was also observed very little histeretic behaviour. These characteristics of high relative amplitude of contraction, little hysteresis, and high power density are one of the main reasons why these fibers are being thoroughly studied (de Almeida et al., 2018), (Sutton et al., 2016), (Cho et al., 2016), (Arakawa et al., 2016), (Yip and Niemeyer, 2017), (de Araújo et al., 2019).

An effective method for heating these coiled polymer actuators (CPAs) was shown by Yip and Niemeyer (2017) to be Joule effect heating. However, when lead to expand by means of only convection and conduction cooling, the response is slow. An alternative would be to use an antagonistic CPA. The work of de Araújo et al. (2019) proposes the use of an antagonistic pair of CPAs to control a rotational joint.

This work is the continuity of the work presented in de Araújo et al. (2019). In the work of de Araújo et al. (2019), a machine for the CPA manufacture is presented, a new thermoelectric model for the CPA is suggested, a nonlinear solver-baser optimization algorithm to identify the parameters for a nonlinear thermomechanical model is used, and the model of a joint driven by antagonists CPAs is developed. However, there was not much attention to the physical meaning of the estimated parameters. Furthermore, the proposed model for the joint did not consider any form of friction for the rotating motion.

In this work, the project of a physical rotating joint is made, and the joint is built. In addition, a different strategy to identify the the CPA thermomechanical model parameters is taken, and a viscous friction component is added to the joint model. The different strategy for the thermomechanical model identification relies on two different experiments designed to gather data relevant to a specific characteristic of the model.

2. CPA MODEL

The mathematical models used for the CPAs were the same as the ones discussed in de Araújo et al. (2019), in which there is a thermoelectric model used for the temperature rise of the fiber due to Joule heating, and a thermomechanical model for the contraction that occurs when a strained CPA is heated. The Joule heating is provided by an enameled copper wire, that is wrapped around the actuator, when subjected to an electric current.

2.1 Thermoelectric model

The differential equation that describes the actuator temperature is shown in (1), in which C is the thermal capacity (J/°C), T is the temperature, i is the current, r_e is the electrical resistance of the copper wire, T_a is the ambient temperature and G is the thermal conductivity.

$$C\dot{T} = i^2 r_e(T) - G(T)(T - T_a) \tag{1}$$

The wire resistance is considered to be variant with temperature as in a first order model. This model for the

[⋆] This work was supported by PPgEE/UFCG and CAPES.

conductor resistance, in terms of the thermoelectric model for the CPA, was proposed by de Almeida et al. (2018), and is shown in (2). In this model, r_0 is the resistance at ambient temperature (T_a), and α is the wire temperature coefficient.

$$r_e(T) = r_0[1 + \alpha(T - T_a)] \tag{2}$$

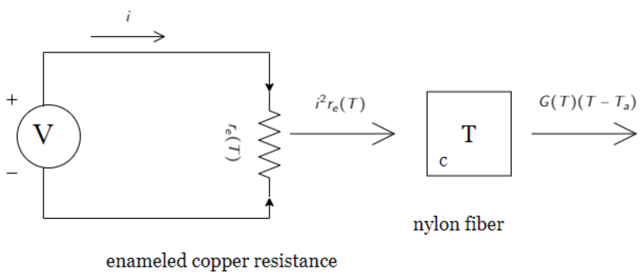

Figure 1. Diagram for the thermoelectric model.

Moreover, the thermal conductivity G was observed by de Araújo et al. (2019) to be variant with temperature and was approximated to a first order model, as shown in (3). In this model, the constant parameter of G is G_0 (W/°C), and the temperature dependent parameter of G is G_1 (W/°C^2).

$$G(T) = G_0 + G_1 T \tag{3}$$

2.2 Thermomechanical model

The thermomechanical model consists of Newton's second law for a mass attached to the actuator free end. A free body diagram for the model is shown in Figure 2. In this model, the mass is subjected to four forces: elastic force (F_K), damping force (F_D), load weight (F_L), and a a force that appears when the actuator is heated (F_T). The mathematical thermomechanical model is shown in 4. The forces F_K and F_T were found to be non-linear by Cho et al. (2016), and were considered by de Araújo et al. (2019) to have the mathematical format shown in (6), and (5), respectively. The equation for the damping force and load weight are shown in (7), and (8) respectively.

$$m\ddot{x} = F_T(T) + F_K(x) - F_L + F_D(\dot{x}) \tag{4}$$

$$F_T(T) = \beta_3(T - T_a)^{\beta_4} \tag{5}$$

$$F_K(x) = \beta_1(x_0 - x)^{\beta_2} \tag{6}$$

$$F_D(\dot{x}) = \beta_5 \dot{x} \tag{7}$$

$$F_L = mg \tag{8}$$

3. ANTAGONISTIC JOINT MODEL

The model for the antagonistic joint was made by applying the models of the antagonistic pair of CPAs to a generic

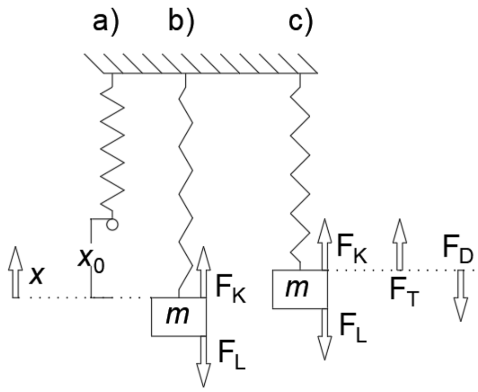

Figure 2. Free-body-diagram of the CPA for the thermo-mechanical model. CPA free of forces a). CPA after being strained by a load of mass m b). CPA being thermally activated c).

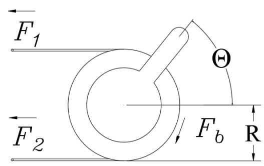

Figure 3. Antagonistic joint forces diagram. The joint is considered to be affected by the antagonistic CPA forces F_1 and F_2, plus some viscous force F_b.

joint model subjected to viscous friction. A diagram for such joint is shown in Figure 3.

The generic joint model consists of Newton's second law applied to a rotational body, and it is mathematically described by (9), in which I is the joint moment of inertia, F_1 is the sum of the elastic force F_{K_1}, and the thermal force F_{T_1} for a CPA; and F_2 is the sum of the elastic force F_{K_2}, and the thermal force F_{T_2} for the antagonistic CPA. F_1, and F_2 are define in (10), and (11) respectively. The damping forces F_D were incorporated in the model for the viscous friction of the joint F_b, which is defined in (12). Note that the parameters for one CPA are annotated as the β symbol, and the parameters for the antagonistic CPA is annotated as the α symbol.

$$F_1(t)R + F_2(t)R - F_b(t)R = I\ddot{\Theta}(t) \tag{9}$$

$$F_1 = \beta_1(x_0 - \Theta R)^{\beta_2} + \beta_3(T_1 - T_a)^{\beta_4} \tag{10}$$

$$F_2 = -\alpha_1(\Theta R + y_0)^{\alpha_2} + \alpha_3(T_2 - T_a)^{\alpha_4} \tag{11}$$

$$F_b = \beta_5\dot{\Theta} + \alpha_5\dot{\Theta} + \frac{b}{R}\dot{\Theta} \tag{12}$$

The elastic forces F_{K_1} and F_{k_2} are defined as (13) and (14) respectively.

$$F_{K_1} = \beta_1(x_0 - \Theta R)^{\beta_2} \tag{13}$$

$$F_{K_2} = -\alpha_1(y_0 + \Theta R)^{\alpha_2} \tag{14}$$

4. PHYSICAL JOINT

In this work, a joint driven by antagonistic CPAs was design and built. The joint was built with purpose to provide data for identification of the joint model parameters and later to be object for a feedback control system. The next subsections provide information about the subsystems designed and the materials used for such.

4.1 Specifications

The specifications for the joint are:

- the joint must be able to perform full rotation of an axis with little or no friction;
- there must be possible to measure the joint angle at a rate of 10 Hz;
- the current that flows through each CPA should be controlled;
- the initial strain of the CPAs can be set.

4.2 Hardware design

In order to meet the specifications, subsystems of hardware were designed and its components specified. A schematic of the proposed joint is shown in Figure 4.

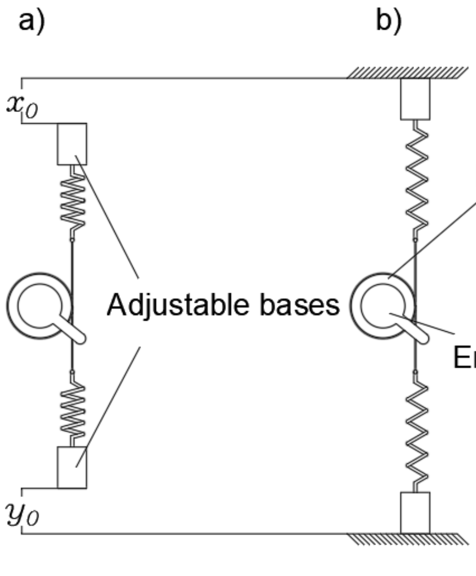

Figure 4. Antagonistic joint schematic. a) CPAs straight but not strained. b) CPAs strained.

4.2.1 Physical structure

The main necessary material consisted in a ball bearing, an encoder, two CPAs, two adjustable bases to each hold one end of a CPA, a microprocessor, a circuit board for data acquisition and signal control, and a support to keep everything together.

The ball bearing must be placed in a way that the outer end is attached to the support, and the inner end is free to rotate. The encoder must be attached to the ball bearing such that it can sense the motion of its rotating end. Each CPA must have one end connected to the rotating part of the bearing and one end connected to an individual base. The bases should be still during the functioning of the joint, but their position should be able do be adjusted as to set the initial strain of the CPAs.

The specific components used to put together the joint physical structure were: a KFL000 bearing; an AS5040 magnetic rotary encoder; an Arduino Mega 2560 board; two 203 mm×163 mm×13 mm plywood boards; a PCB board, for the electrical circuits; two adjustable bases, made with 3D printed parts and M4 screws; a brass axis, to be the joint axis; and a 3D printed base, to accurately position the encoder under the axis.

4.3 Electrical design

An electrical project is necessary to attend the requirements of data acquisition and current control. The AS5040 encoder can provide a 10 bit digital output at a sampling rate of 10 Hz; however, at such rate the output signal is noisy, in a way that decoupling capacitors are required to reduce the noise. The Arduino Mega 2560 control signals are usually PWM signals with amplitude of 5 V; therefore, a circuit must be designed to convert these signals into a current signal of useful range.

The circuit used to convert the Arduino PWM signal into a current signal is shown in Figure 5, and can be thought of as in two stages. The first stage is low pass a filter that averages the PWM signal (the filter parameters are R_f and C_f). The second stage is a voltage to current converter circuit . In this circuit, the induced current i_0 that flows through R is the same that flows through enameled copper (R_c), and is given by

$$i_0 = \frac{V_{av}}{R}, \tag{15}$$

in which V_{av} is the output of the low pass filter. This means that R must be designed as for the maximum value desired for the current i_0 to be $\frac{5}{R}$.

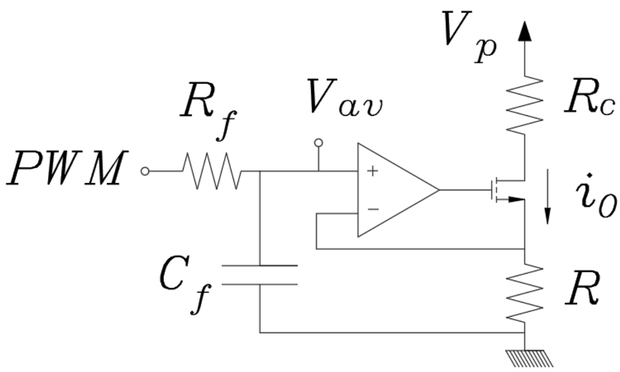

Figure 5. Voltage to current converter circuit.

5. CPA PARAMETER ESTIMATION

The thermoelectric parameters were estimated by the same method as described in de Araújo et al. (2019), so it will not be discussed here. On the other hand, the thermomechanical model parameters were estimated by means of the least squares method performed on data acquired from two different experiments. These experiments were designed to gather data relevant to estimate F_K and F_T.

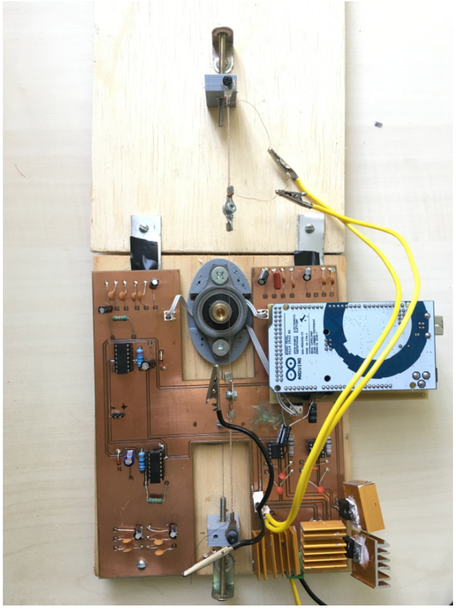

Figure 6. Joint built.

5.1 Thermomechanical model

To be able to identify the parameters β_1, β_2, β_3, and β_4 for the thermomechanical model; two experiments were performed using the platform developed by de Almeida et al. (2018). The first experiment was made to get data for β_1, and β_2 identification; and the second experiment was made to get data to identify β_3, and β_4.

In the first experiment, the upper end of the CPA was fixed, and loads from 0 g to 300 g at a step of 50 g were attached to the CPA, whist its displacement was being measured with an LVDT. The data acquired followed (16) such that g is the gravity, m_i are the loads, x_i are the displacements measured, x_0 is the displacement measured with no load, and $i = 0, 1, 2, 3, 4, 5, 6, 7$.

$$m_i g = \beta_1 (x_0 - x_i)^{\beta_2} \tag{16}$$

Since (16) is not linear in the parameters, the least squares identification method could not be made. So, a natural logarithm was applied in (6), as is shown in (17).

$$\ln(m_i g) = \ln(\beta_1) + \beta_2 \ln(x_0 - x_i) \tag{17}$$

Once we had an equation that was linear in the parameters, the least squares identification method was applied. The results for the identification are shown in Figure 7, in which the dots are the measured displacement for the load applied, and the curve is the estimated model for the elastic force.

This experiment was performed several times in order to improve identification. The variants on the experiments were chosen to be; weather the loads added were putted in an increasing or decreasing manner, and weather the CPA was strained, at rest, or was heated up right before the experiment. On Figure 7, the measured data was obtained when the experiment was performed in the following form, respectively:

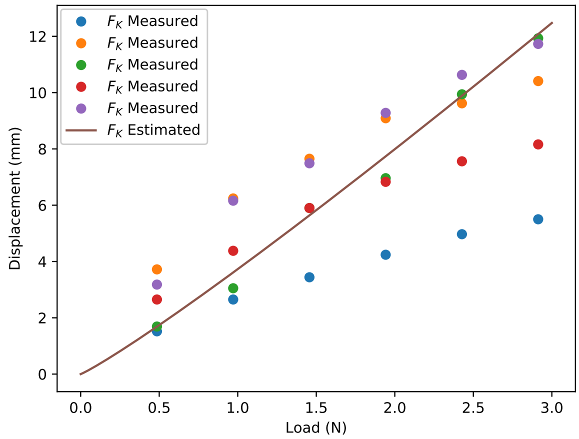

Figure 7. Relationship between elastic force and displacement $(x_0 - x)$. Cost function error is $V(F_K) = 3.84779585$ N^2.

- experiment with decreasing load after cycles of active heating and convection cooling;
- experiment with decreasing load after a couple hours strained;
- experiment with increasing load after a couple hours at rest;
- experiment with decreasing load after having both ends fixed and the CPA subjected to a staircase current signal;
- experiment with decreasing load after a couple hours strained.

Seeing, from Figure 7, that the parameters for the elastic force appear to significantly change, and that there is an insufficient number of data, no data was used for validation. Instead, the identified model was used as base line for further identification, as will be shown in Section 6.

In the second experiment, the CPA was strained and fixed. The upper end of the CPA was attached to a load cell, and the lower end of the CPA was attached to a fixed point. Afterwards a repeating staircase current signal was sent in order to slowly increase the CPA temperature. While the signal was being sent, the CPA temperature and force was being measured by means of a micro thermocouple and the load cell. The whole data was recorded at a sampling rate of 10 Hz, and is shown in Figure 8.

Since there was no contraction, the load cell was only sensitive to F_K, and F_T. In this configuration, F_K was constant, so in order to obtain only we subtracted the initial measured force (F_K) from the force being measured (F_{lc}), as is shown in 18.

$$F_{lc} - F_K = F_T(T) \tag{18}$$

Similarly to (16), a natural logarithm was applied to equation (18) to make it linear in the parameters, so the least squares could be used, as is shown in (19). In the second experiment, 80% of the data were used for identification and 20% for validation. The curves of $F_T(T)$ measured, estimated and validated are shown in Figure 9.

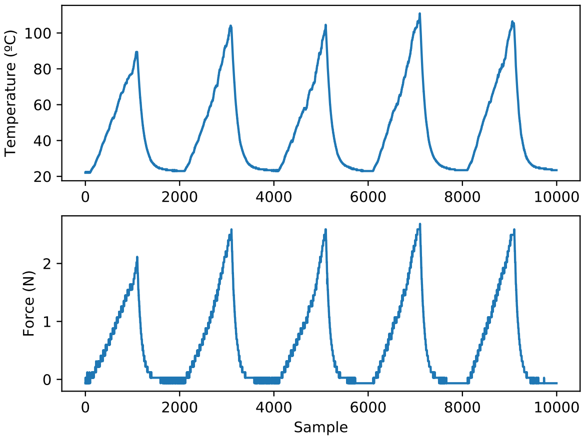

Figure 8. Data of temperature (T) and force- $F_{T(T)}$ from the second experiment.

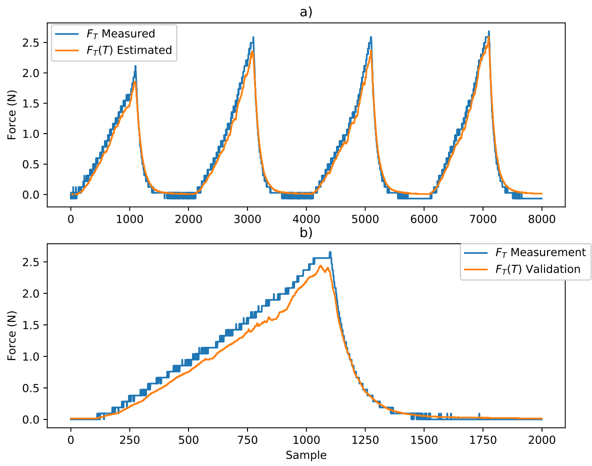

Figure 9. a) Measured and estimated F_T curve. b) Curves of F_T for validation. Cost function error is $V(F_T) = 42.74382147$ N^2.

$$\ln(F_{lc} - F_K) = \ln(\beta_3) + \beta_4 \ln(T_j - T_a) \tag{19}$$

Since the joint is controlled by two CPAs, the parameter estimation was performed for two different CPAs. The parameters β, and α estimated are shown in Table 1.

Table 1. Thermomechanical parameters.

β_i,$i = 1, 2, 3, 4$	Value	α_i, $i = 1, 2, 3, 4$	Value
β_1	161.9783	α_1	116.4304
β_2	0.9099	α_2	0.8374
β_3	0.0108	α_3	0.0163
β_4	1.2225	α_4	1.1076

6. JOINT PARAMETER ESTIMATION

To gather data for the joint model parameters identification an experiment involving the joint built in this work. This experiment consisted first in attach the two CPAs manufactured (and whose models were previously estimated) to the joint. Afterwards, two alternating pulsed current signals were sent to the actuators. The current signals had 200 seconds period and 50% duty-cycle. In this experiment, the signals of current were taken to be as in 15. Moreover, during the experiment the values of θ were recorded at 10 Hz sampling period. The data from the experiment is shown in Figure 10. In addition, even though the CPAs temperatures were not measured, they were estimated by means of the thermoelectric model.

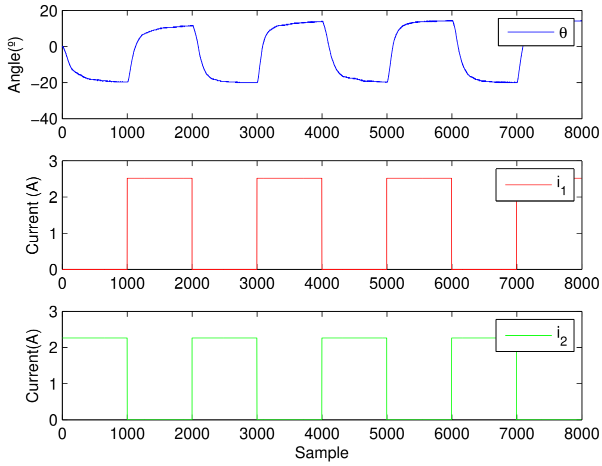

Figure 10. Recorded data from the joint experiment

Because both CPA and joint are considered to be affected by viscous friction, for convenience, only one parameter associated with viscous friction was estimated. So (12) was considered as in (20), in which $\bar{b}$ is given as in (21).

$$F_b = \bar{b}\dot{\Theta} \tag{20}$$

$$\bar{b} = \beta_5 + \alpha_5 + b \tag{21}$$

It was observed that by taking off the load from a strained CPA and waiting a few hours, the CPA parameters could slightly change if the parameter estimation experiments were performed again, as can be seen in Figure 7. So, in order to obtain an optimal mathematical model for the joint, but with its parameter values close to the ones previous estimated, a non linear optimization algorithm was used.

The equation from which the parameters were estimated was the Newton's second law applied to a rotating body, equation (9). Since the algorithm works with discrete models, the equation (9) was discretized by means of the forward Euler finite difference method, which after solving for $\theta_{[k]}$ resulted in (22).

$$\begin{aligned}\theta_{[k]} =& \frac{Rh^2}{I}(\beta_1(x_0 - \theta_{[k-2]}R)^{\beta_2} + \beta_3(T_{1[k-2]} - T_a)^{\beta_4} \\ & - \alpha_1(y_0 + \theta_{[k-2]}R)^{\alpha_2} - \alpha_3(T_{2[k-2]} - T_a)^{\alpha_4}) \\ & + \theta_{[k-1]}(2 - \frac{\bar{b}hR}{I}) + \theta_{[k-2]}(\frac{\bar{b}hR}{I} - 1)\end{aligned} \tag{22}$$

Since the CPAs parameters are likely to vary, when they are removed from the platform and installed in the joint, the parameters β_1, β_2, β_3, and β_4 were re estimated. The used algorithm solves the error magnitude function described in (23), in which $\hat{\theta}$ are the estimated values of θ given by (24), and p is a vector of the parameters to be estimated, as is shown in (25).

$$\hat{p} = \underset{p \in \mathbb{D}}{\operatorname{argmin}} \frac{1}{2} \sum_{k=1}^{K} \left[\theta_{[k]} - \hat{\theta}_{[k]}(p) \right]^2, \mathbb{D} \subseteq \mathbb{R}^{10}_{>0} \tag{23}$$

$$\begin{aligned} \hat{\theta}_{[k]} = & \frac{Rh^2}{p_{10}} (p_1 (x_0 - \theta_{[k-2]} R)^{p_2} + p_3 (T_{1[k-2]} - T_a)^{p_4} \\ & - p_5 (y_0 + \theta_{[k-2]} R)^{p_6} - p_7 (T_{2[k-2]} - T_a)^{p_8}) \\ & + \theta_{[k-1]} (2 - \frac{p_9 h R}{I}) + \theta_{[k-2]} (\frac{p_9 h R}{I} - 1) \end{aligned} \tag{24}$$

$$p = [p_1 \; p_2 \; p_3 \; p_4 \; p_5 \; p_6 \; p_7 \; p_8 \; p_9 \; p_{10}] \tag{25}$$

As was previously mentioned, the idea is to obtain the parameters I, β_1, β_2, β_3, and β_4 close to their values firstly estimated. To do so, initial values, lower bounds and upper bound were given to p, as it is shown respectively in (26), (27), and(28).

The initial value for the moment of inertia $\overline{I}$ was calculated considering the rotating part of the joint as being a perfect solid cylinder; however, since that is not case, the moment of inertia was also taken as an estimated parameter. The initial value for the β and α were taken to be the values previously estimated.

The lower and upper bounds for the inertia moment were arbitrarily chosen to be a 10% variation of the initial value. The lower and upper bounds for β_1, β_2, α_1, and α_2 were chosen to be the initial value added and subtracted by the standard deviation of the estimated β (σ) and α (δ) per experiment. The curves of the measured θ and estimated model are shown in Figure 11, and the curves of the measured θ and validated model are shown in Figure 12. Finally, the values for the re estimated parameters β, and α are shown in Table 2, and the values for the estimated moment of inertia and viscous friction are shown in Table 3.

$$p_0 = [\hat{\beta}_1 \; \hat{\beta}_2 \; \hat{\beta}_3 \; \hat{\beta}_4 \; \hat{\alpha}_1 \; \hat{\alpha}_2 \; \hat{\alpha}_3 \; \hat{\alpha}_4 \; 0 \; \overline{I}] \tag{26}$$

$$p_{lb} = [\hat{\beta}_1 - \sigma_1 \; \hat{\beta}_2 - \sigma_2 \; 0 \; 0 \; \hat{\alpha}_1 - \delta_1 \; \hat{\alpha}_2 - \delta_2 \; 0 \; 0 \; 0 \; \overline{I} \times 0.9] \tag{27}$$

$$p_{ub} = [\hat{\beta}_1 + \sigma_1 \; \hat{\beta}_2 + \sigma_2 \; \infty \; \infty \; \hat{\alpha}_1 + \delta_1 \; \hat{\alpha}_2 + \delta_2 \; \infty \; \infty \; \infty \; \overline{I} \times 1.1] \tag{28}$$

Table 2. Thermomechanical parameters.

β_i, $i = 1, 2, 3, 4$	Value	α_i, $i = 1, 2, 3, 4$	Value
β_1	165.0101	α_1	119.4447
β_2	0.8045	α_2	0.7455
β_3	0.0089	α_3	0.0021
β_4	1.0631	α_4	1.4911

7. CONCLUSION

In this work, a project for a rotational joint controlled by antagonistic CPAs was made and executed. Furthermore, thermomechanical models were estimated for the actuators by gathering data from two different experiments and using the least squares identification method. Afterwards, the identification of the joint model was made by gathering data from a dynamic experiment with the joint, using the previous estimated CPAs parameters, and applying a non linear optimization algorithm.

As for future work, a control law based on the identified model will be designed, tested, and its performance will be evaluated.

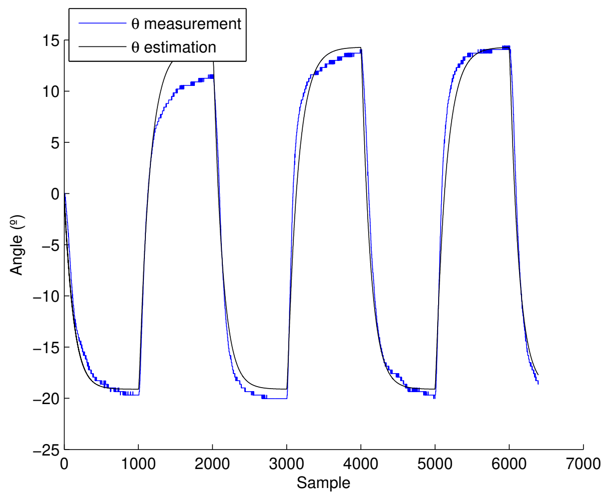

Figure 11. Joint model estimation curve. Cost function value $V(\theta) = 1.0127$ rad^2.

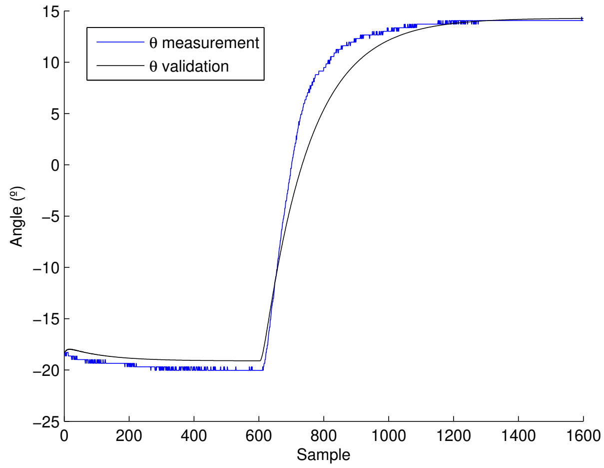

Figure 12. Joint model validation curve.

Table 3. Joint parameters.

Parameter	Value
I	8.8122e-04 kg.m^2
$\overline{b}$	8.0111e-04 N.m.s/rad

ACKNOWLEDGEMENTS

The authors acknowledge and thank the financial support provided by PPgEE/UFCG, CAPES and CNPq.

REFERENCES

Arakawa, T., Takagi, K., Tahara, K., and Asaka, K. (2016). Position control of fishing line artificial muscles (coiled polymer actuators) from nylon thread. In *Conf. Rec. SPIE/EAPAD*.

Cho, K.H., Song, M.G., Jung, H., Yang, S.Y., Moon, H., Koo, J.C., Choi, H.R., et al. (2016). Fabrication and modeling of temperature-controllable artificial muscle actuator. In *Conf. Rec. IEEE/BioRob*.

de Almeida, K.C.B., Luiz, S.O.D., Lima, A.M.N., and de Araújo, J.R.C. (2018). Experimental platform for characterizing a nylon thread thermomechanical actuator. In *Anais do XXII CBA*.

de Araújo, J.R.C., Luiz, S.O.D., and Lima, A.M.N. (2019). Polymer fiber actuators: manufacturing, modeling and application on an antagonistic joint. In *Anais do XIV SBAI*.

Haines, C.S., Lima, M.D., Li, N., Spinks, G.M., Foroughi, J., Madden, J.D., Kim, S.H., Fang, S., de Andrade, M.J., Göktepe, F., et al. (2014). Artificial muscles from fishing line and sewing thread. *Science*.

Sutton, L., Moein, H., Rafiee, A., Madden, J.D., and Menon, C. (2016). Design of an assistive wrist orthosis using conductive nylon actuators. In *Conf. Rec. IEEE/BioRob*.

Yip, M.C. and Niemeyer, G. (2017). On the control and properties of supercoiled polymer artificial muscles. *IEEE Transactions on Robotics*.